

VIETNAM ACADEMY OF SCIENCE AND TECHNOLOGY

Vietnam Journal

of MECHANICS

Volume 35 Number 1

ISSN 0866-7136

VN INDEX 12.666

1
2013
35th Anniversary

POSTBUCKLING OF FUNCTIONALLY GRADED CYLINDRICAL SHELLS BASED ON IMPROVED DONNELL EQUATIONS

Dao Huy Bich¹, Nguyen Xuan Nguyen¹, Hoang Van Tung²

¹*Hanoi University of Science, VNU, Vietnam*

²*Hanoi Architectural University, Vietnam*

Abstract. This paper presents an analytical approach to investigate the buckling and postbuckling of functionally graded cylindrical shells subjected to axial and transverse mechanical loads incorporating the effects of temperature. Material properties are assumed to be temperature independent, and graded in the thickness direction according to a simple power law distribution in terms of the volume fractions of constituents. Equilibrium equations for perfect cylindrical shells are derived by using improved Donnell shell theory taking into account geometrical nonlinearity. One-term approximate solution is assumed to satisfy simply supported boundary conditions and closed-form expressions of buckling loads and load-deflection curves are determined by Galerkin method. Analysis shows the effects of material and the geometric parameters, buckling mode, pre-existent axial compressive and thermal loads on the nonlinear response of the shells.

Keywords: Postbuckling, functionally graded materials, cylindrical shells, improved Donnell theory, temperature effects.

1. INTRODUCTION

Cylindrical shell is one of the most common structures found in many applications of various industries. As a result, problems relating to the stability including buckling and postbuckling behaviors of this type of shell have a major importance for safe and reliable design and attract attention of many researchers. Brush and Almroth [1] introduced an excellent work on buckling of bars, plates and shells in which linear stability of cylindrical shell structures under basic types of loading has been analyzed. However, the results were mainly presented for isotropic shallow cylindrical shells. Birman and Bert [2] investigated dynamic stability of reinforced composite cylindrical shells subjected to pulsating loads acting in the axial direction and in the presence of a thermal field on the basis of Donnell theory for laminated shells and a linear analysis. They then considered the buckling and postbuckling behaviors of reinforced cylindrical shells subjected to the simultaneous action of a thermal field and an axial loading by using improved version of Donnell theory ignoring the shallowness of cylindrical shells [3]. Their paper also formulated conditions for the snap-through of a cylindrical shell under thermomechanical loading. Eslami et al. [4] established improved stability equations for linear buckling analysis of isotropic short

and long cylindrical shells under thermal loadings. An analytical approach was used in above mentioned studies.

Due to advanced characteristics in comparison with traditional metals and conventional composites, Functionally Graded Materials (FGMs) consisting of metal and ceramic constituents have received increasingly attention in structural applications in recent years. Smooth and continuous change in material properties enable FGMs to avoid interface problems and unexpected thermal stress concentrations. By high performance heat resistance capacity, FGMs are now chosen to use as structural components exposed to severe temperature conditions such as aircraft, aerospace structures, nuclear plants and other engineering applications. Shahsiah and Eslami [5] employed Donnell shell theory and coupled form of stability equations to study linear buckling of simply supported FGM shallow cylindrical shells under thermal loads. Subsequently, they extended this analytical approach for FGM nonshallow long cylindrical shells [6] in which improved terms of the classical thin shell theory were incorporated. Lanhe et al. [7] utilized the Donnell theory, uncoupled form of stability equation and one-term approximate solution to determine closed-form expressions of critical temperatures for simply supported FGM cylindrical shells. Buckling behavior of cylindrical shells with FGM middle layer, imperfect FGM cylindrical shells and FGM stiffened cylindrical shells under axial compressive load were analytically investigated in works [8-10], respectively. Postbuckling behavior of FGM cylindrical shells has been presented in some studies. Shen [11] investigated thermal postbuckling of simply supported FGM cylindrical shells under uniform temperature rise. He used the classical shell theory, boundary layer theory of shell buckling and asymptotic perturbation technique to determine critical temperatures and postbuckling temperature-deflection curves with both geometric imperfection and temperature dependence of material properties are taken into consideration. Following this direction, thermomechanical postbuckling behaviors of FGM cylindrical shells with and without piezoelectric layer were also reported in works [12-14]. By using analytical method and the classical theory, nonlinear buckling and postbuckling of FGM cylindrical shells under axial compression and combined mechanical loads have been considered by Huang and Han [15, 16]. Recently, Darabi et al. [17] presented an analytical study on the nonlinear dynamic stability of simply supported FGM circular cylindrical shells under periodic axial loading. Also, nonlinear dynamic stability of FGM cylindrical shells with and without piezoelectric layers under thermomechanical and thermo-electro-mechanical loads has been treated by Shariyat [18,19]. He employed a high-order shell theory proposed by Shariyat and Eslami [20] in which transverse shear stress influences are also included, finite element method and a two-step iterative method to determine buckling loads and postbuckling curves. It is excepted for works [3, 4, 6], most of aforementioned investigations used the theories in which the shallowness of cylindrical shells is assumed. This results from the complexity of basic equations when assumption on the shallowness is ignored due to difficulty in defining a suitable stress function. However, improved terms should be included in the shell theories for more exact predictions, especially nonshallow long cylindrical shells.

In this paper, buckling and postbuckling behaviors of FGM cylindrical shells under mechanical loads with and without temperature effects are investigated by an analytical approach. Equilibrium equations are established by using improved Donnell shell theory

with kinematic nonlinearity is taken into consideration. One-term approximate solution satisfying simply supported boundary conditions is assumed and closed-form expressions of buckling loads and nonlinear load-deflection curves are determined by Galerkin method. The effects of material and geometric parameters, buckling mode, pre-existent axial compressive and thermal loads on the stability of FGM cylindrical shells are considered and discussed.

2. FUNCTIONALLY CYLINDRICAL SHELLS

Consider a functionally graded circular cylindrical shell of radius of curvature R , thickness h and length L as shown in Fig. 1. The shell is made from a mixture of ceramics and metals and is defined in coordinate system (x, θ, z) , where x and θ are in the axial and circumferential directions of the shell, respectively, and z is perpendicular to the middle surface and points outwards ($-h/2 \leq z \leq h/2$).

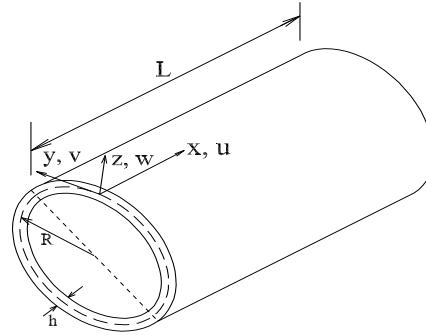


Fig. 1. Configuration and the coordinate system of a cylindrical shell

Suppose that the material composition of the shell varies smoothly along the thickness is such a way the inner surface is metal-rich and the outer surface is ceramic-rich by following a simple power law in terms of the volume fractions of the constituents as

$$V_c(z) = \left(\frac{2z + h}{2h} \right)^k, \quad V_m(z) = 1 - V_c(z) \quad (1)$$

where V_c and V_m are the volume fractions of ceramic and metal constituents, respectively, and volume fraction index k is a nonnegative number that defines the material distribution. It is assumed that the effective properties Pr_{eff} of FGM cylindrical shell change in the thickness direction z and can be determined by the linear rule of mixture as

$$Pr_{eff}(z) = Pr_c V_c(z) + Pr_m V_m(z) \quad (2)$$

where Pr denotes a temperature-independent material property, and subscripts m and c represent the metal and ceramic constituents, respectively.

From Eqs. (1) and (2) the effective properties of FGM cylindrical shell such as modulus of elasticity E , the coefficient of thermal expansion α , and the coefficient of

thermal conduction K can be defined as

$$[E(z), \alpha(z), K(z)] = [E_m, \alpha_m, K_m] + [E_{cm}, \alpha_{cm}, K_{cm}] \left(\frac{2z+h}{2h} \right)^k \quad (3)$$

whereas Poisson ratio ν is assumed to be constant and

$$E_{cm} = E_c - E_m, \alpha_{cm} = \alpha_c - \alpha_m, K_{cm} = K_c - K_m. \quad (4)$$

It is evident that $E = E_c$, $\alpha = \alpha_c$, $K = K_c$ at $z = h/2$ and $E = E_m$, $\alpha = \alpha_m$, $K = K_m$ at $z = -h/2$.

3. GOVERNING EQUATIONS

In the present study, the improved Donnell shell theory is used to obtain the equilibrium equations as well as expressions of buckling loads and nonlinear load-deflection curves of FGM cylindrical shells. The strains across the shell thickness at a distance z from the middle surface are

$$\varepsilon_x = \varepsilon_{x0} + zk_x, \varepsilon_y = \varepsilon_{y0} + zk_y, \gamma_{xy} = \gamma_{xy0} + zk_{xy} \quad (5)$$

where ε_{x0} and ε_{y0} are the normal strains, γ_{xy0} is the shear strain at the middle surface of the shell, whereas k_x , k_y , k_{xy} are the change of curvatures and twist. According to Sanders assumption, the strains at the middle surface and the change of curvatures and twist are related to the displacement components u , v , w in the x , y , z coordinate directions, respectively, as [1]

$$\begin{aligned} \varepsilon_{x0} &= u_{,x} + \frac{1}{2}w_{,x}^2, \quad \varepsilon_{y0} = v_{,y} - \frac{w}{R} + \frac{1}{2}w_{,y}^2, \quad \gamma_{xy0} = u_{,y} + v_{,x} + w_{,x}w_{,y} \\ k_x &= -w_{,xx}, \quad k_y = -w_{,yy} - \frac{1}{R}v_{,y}, \quad k_{xy} = -w_{,xy} - \frac{1}{2R}v_{,x} \end{aligned} \quad (6)$$

where $y = R\theta$ and subscript $(,)$ indicates the partial derivative.

Hooke law for a functionally graded cylindrical shell including temperature effects is defined as

$$\begin{aligned} (\sigma_x, \sigma_y) &= \frac{E}{1-\nu^2} [(\varepsilon_x, \varepsilon_y) + \nu(\varepsilon_y, \varepsilon_x) - (1+\nu)\alpha\Delta T(1, 1)] \\ \sigma_{xy} &= \frac{E}{2(1+\nu)}\gamma_{xy}, \end{aligned} \quad (7)$$

where ΔT denotes the change of environment temperature from stress free initial state or temperature difference between the surfaces of FGM cylindrical shell.

The force and moment resultants of an FGM cylindrical shell are expressed in terms of the stress components through the thickness as

$$(N_{ij}, M_{ij}) = \int_{-h/2}^{h/2} \sigma_{ij}(1, z)dz, \quad ij = x, y, xy. \quad (8)$$

Introduction of Eqs. (3), (5) and (7) into Eqs. (8) gives the constitutive relations in the matrix form as

$$\begin{bmatrix} N_x \\ N_y \\ N_{xy} \\ M_x \\ M_y \\ M_{xy} \end{bmatrix} = \begin{bmatrix} A_{11} & A_{12} & 0 & B_{11} & B_{12} & 0 \\ A_{12} & A_{22} & 0 & B_{12} & B_{22} & 0 \\ 0 & 0 & A_{66} & 0 & 0 & B_{66} \\ B_{11} & B_{12} & 0 & D_{11} & D_{12} & 0 \\ B_{12} & B_{22} & 0 & D_{12} & D_{22} & 0 \\ 0 & 0 & B_{66} & 0 & 0 & D_{66} \end{bmatrix} \begin{bmatrix} \varepsilon_{x0} \\ \varepsilon_{y0} \\ \gamma_{xy0} \\ k_x \\ k_{xy} \\ 2k_{xy} \end{bmatrix} - \begin{bmatrix} \Phi_0/(1-\nu) \\ \Phi_0/(1-\nu) \\ 0 \\ \Phi_1/(1-\nu) \\ \Phi_1/(1-\nu) \\ 0 \end{bmatrix} \quad (9)$$

where

$$\begin{aligned} A_{11} = A_{22} &= \frac{E_1}{1-\nu^2}, \quad A_{12} = \nu A_{11}, \quad A_{66} = \frac{E_1}{2(1+\nu)} \\ B_{11} = B_{22} &= \frac{E_2}{1-\nu^2}, \quad B_{12} = \nu B_{11}, \quad B_{66} = \frac{E_2}{2(1+\nu)} \\ D_{11} = D_{22} &= \frac{E_3}{1-\nu^2}, \quad D_{12} = \nu D_{11}, \quad D_{66} = \frac{E_3}{2(1+\nu)} \end{aligned} \quad (10)$$

and

$$\begin{aligned} E_1 &= E_m h + E_{cm} h / (k+1), \quad E_2 = E_{cm} h^2 [1/(k+2) - 1/(2k+2)] \\ E_3 &= E_m h^3 / 12 + E_{cm} h^3 [1/(k+3) - 1/(k+2) + 1/(4k+4)], \\ (\Phi_0, \Phi_1) &= \int_{-h/2}^{h/2} \left[E_m + E_{cm} \left(\frac{2z+h}{2h} \right)^k \right] \left[\alpha_m + \alpha_{cm} \left(\frac{2z+h}{2h} \right)^k \right] \Delta T(1, z) dz \end{aligned} \quad (11)$$

The nonlinear equilibrium equations of a perfect cylindrical shell based on the improved Donnell shell theory are

$$\begin{aligned} N_{x,x} + N_{xy,y} &= 0 \\ N_{xy,x} + N_{y,y} - \frac{1}{R} (M_{xy,x} + M_{y,y}) &= 0 \\ M_{x,xx} + 2M_{xy,xy} + M_{y,yy} + \frac{N_y}{R} + N_x w_{,xx} + 2N_{xy} w_{,xy} + N_y w_{,yy} \\ &\quad + (N_{xy,x} + N_{y,y}) w_{,y} - P_x h w_{,xx} + q = 0 \end{aligned} \quad (12)$$

where P_x is axial uniform compressive force acting on two ends of the shell and q is external pressure uniformly distributed on the surface of the shell.

Substituting of Eqs. (6) into Eqs. (9) and then into Eqs. (12), the system of equilibrium equations (12) is rewritten in terms of displacement components as follows

$$\begin{aligned} L_{11}(u) + L_{12}(v) - L_{13}(w) + P_1(w) &= 0 \\ L_{21}(u) + L_{22}(v) - L_{23}(w) + P_2(w) &= 0 \\ L_{31}(u) + L_{32}(v) - L_{33}(w) + P_3(w) + Q_3(u, w) + R_3(v, w) \\ &\quad - \frac{\Phi_0}{1-\nu} \left(w_{,xx} + w_{,yy} + \frac{1}{R} \right) - P_x h w_{,xx} + q = 0 \end{aligned} \quad (13)$$

where linear operators $L_{ij}()$ ($i, j = 1, 2, 3$) and nonlinear operators $P_i()$ ($i = 1, 2, 3$), $Q_3(,)$, $R_3(,)$ are defined as follows

$$\begin{aligned}
L_{11}() &= A_{11} \frac{\partial^2}{\partial x^2} + A_{66} \frac{\partial^2}{\partial y^2} \\
L_{12}() = L_{21}() &= \left(A_{12} + A_{66} - \frac{B_{12} + B_{66}}{R} \right) \frac{\partial^2}{\partial x \partial y} \\
L_{13}() = L_{31}() &= \frac{A_{12}}{R} \frac{\partial}{\partial x} + B_{11} \frac{\partial^3}{\partial x^3} + (B_{12} + 2B_{66}) \frac{\partial^3}{\partial x \partial y^2} \\
L_{22}() &= \left(A_{66} - \frac{2B_{66}}{R} + \frac{D_{66}}{R^2} \right) \frac{\partial^2}{\partial x^2} + \left(A_{11} - \frac{2B_{11}}{R} + \frac{D_{11}}{R^2} \right) \frac{\partial^2}{\partial y^2} \\
L_{23}() = L_{32}() &= \left(\frac{A_{11}}{R} - \frac{B_{11}}{R^2} \right) \frac{\partial}{\partial y} + \left(B_{11} - \frac{D_{11}}{R} \right) \frac{\partial^3}{\partial y^3} \\
&\quad + \left(B_{12} + 2B_{66} - \frac{D_{12} + 2D_{66}}{R} \right) \frac{\partial^3}{\partial x^2 \partial y} \\
L_{33}() &= \frac{A_{11}}{R^2}() + \frac{2B_{12}}{R} \frac{\partial^2}{\partial x^2} + \frac{2B_{11}}{R} \frac{\partial^2}{\partial y^2} + D_{11} \left(\frac{\partial^4}{\partial x^4} + \frac{\partial^4}{\partial y^4} \right) \\
&\quad + 2(D_{12} + 2D_{66}) \frac{\partial^4}{\partial x^2 \partial y^2} \\
P_1() &= A_{11} \frac{\partial}{\partial x} \frac{\partial^2}{\partial x^2} + (A_{12} + A_{66}) \frac{\partial}{\partial y} \frac{\partial^2}{\partial x \partial y} + A_{66} \frac{\partial}{\partial x} \frac{\partial^2}{\partial y^2} \\
P_2() &= \left(A_{66} - \frac{B_{66}}{R} \right) \frac{\partial^2}{\partial x^2} \frac{\partial}{\partial y} + \left(A_{11} - \frac{B_{11}}{R} \right) \frac{\partial}{\partial y} \frac{\partial^2}{\partial y^2} \\
&\quad + \left(A_{12} + A_{66} - \frac{B_{12} + B_{66}}{R} \right) \frac{\partial}{\partial x} \frac{\partial^2}{\partial x \partial y} \\
P_3(w) &= -\frac{w}{R} \left(A_{12} \frac{\partial^2 w}{\partial x^2} + A_{11} \frac{\partial^2 w}{\partial y^2} \right) + 2(B_{66} - B_{12}) \frac{\partial^2}{\partial x^2} \frac{\partial^2}{\partial y^2} \\
&\quad + 2(B_{12} - B_{66}) \left(\frac{\partial^2 w}{\partial x \partial y} \right)^2 - \frac{A_{12}}{2R} \left(\frac{\partial w}{\partial x} \right)^2 - \frac{A_{11}}{2R} \left(\frac{\partial w}{\partial y} \right)^2 \\
&\quad + \frac{3A_{11}}{2} \left[\frac{\partial^2 w}{\partial x^2} \left(\frac{\partial w}{\partial x} \right)^2 + \frac{\partial^2 w}{\partial y^2} \left(\frac{\partial w}{\partial y} \right)^2 \right] + 2(A_{12} + 2A_{66}) \frac{\partial w}{\partial x} \frac{\partial w}{\partial y} \frac{\partial^2}{\partial x \partial y} \\
&\quad + \left(\frac{A_{12}}{2} + A_{66} \right) \left[\frac{\partial^2 w}{\partial y^2} \left(\frac{\partial w}{\partial x} \right)^2 + \frac{\partial^2 w}{\partial x^2} \left(\frac{\partial w}{\partial y} \right)^2 \right] \\
Q_3(u, w) &= A_{11} \left(\frac{\partial u}{\partial x} \frac{\partial^2 w}{\partial x^2} + \frac{\partial^2 u}{\partial x^2} \frac{\partial w}{\partial x} \right) + A_{12} \frac{\partial u}{\partial x} \frac{\partial^2 w}{\partial y^2} + A_{66} \frac{\partial^2 u}{\partial y^2} \frac{\partial w}{\partial x} \\
&\quad + (A_{12} + A_{66}) \frac{\partial^2 u}{\partial x \partial y} \frac{\partial w}{\partial y} + 2A_{66} \frac{\partial u}{\partial y} \frac{\partial^2 w}{\partial x \partial y}
\end{aligned} \tag{14}$$

$$\begin{aligned}
R_3(v, w) = & \left(A_{12} - \frac{B_{12}}{R} \right) \frac{\partial v}{\partial y} \frac{\partial^2 w}{\partial x^2} + \left(A_{66} - \frac{B_{66}}{R} \right) \left[2 \frac{\partial v}{\partial x} \frac{\partial^2 w}{\partial x \partial y} + \frac{\partial^2 v}{\partial x^2} \frac{\partial w}{\partial y} \right] \\
& + \left(A_{11} - \frac{B_{11}}{R} \right) \left[\frac{\partial v}{\partial y} \frac{\partial^2 w}{\partial y^2} + \frac{\partial^2 v}{\partial y^2} \frac{\partial w}{\partial y} \right] \\
& + \left(A_{12} + A_{66} - \frac{B_{12} + B_{66}}{R} \right) \frac{\partial^2 v}{\partial x \partial y} \frac{\partial w}{\partial x}.
\end{aligned}$$

In what follows, specific expressions of thermal parameter Φ_0 for two types of thermal loads will be determined.

3.1. Uniform temperature rise

Environment temperature can be raised from initial value T_i to final one T_f and temperature difference $\Delta T = T_f - T_i$ is a constant. In this case, the thermal parameter Φ_0 can be expressed in terms of the ΔT from Eqs. (11) as follows

$$\Phi_0 = I \Delta T h, \quad I = E_m \alpha_m + \frac{E_m \alpha_{cm} + E_{cm} \alpha_m}{k + 1} + \frac{E_{cm} \alpha_{cm}}{2k + 1} \quad (15)$$

3.2. Through the thickness temperature gradient

In this case, the temperature through the thickness is governed by the one-dimensional Fourier equation of steady-state heat conduction established in cylindrical coordinate system whose origin is on the symmetric axis of cylinder rather than on the middle surface of cylindrical shell

$$\frac{d}{d\bar{z}} \left[K(\bar{z}) \frac{dT}{d\bar{z}} \right] + \frac{K(\bar{z})}{\bar{z}} \frac{dT}{d\bar{z}} = 0, \quad T(\bar{z} = R - h/2) = T_m, \quad T(\bar{z} = R + h/2) = T_c \quad (16)$$

where T_c and T_m are temperatures at ceramic-rich and metal-rich surfaces, respectively. In Eq. (16), \bar{z} is radial coordinate of a point which is distant z from the shell middle surface with respect to the symmetric axis of cylinder, i.e. $\bar{z} = R + z$ and $R - h/2 \leq \bar{z} \leq R + h/2$.

The solution of Eq. (16) can be expressed as follows

$$T(\bar{z}) = T_m + \frac{\Delta T}{R+h/2} \int_{\int_{R-h/2}^{\bar{z}} \frac{d\bar{z}}{\bar{z}K(\bar{z})} R-h/2}^{\bar{z}} \frac{d\zeta}{\zeta K(\zeta)} \quad (17)$$

where, in this case, $\Delta T = T_c - T_m$ is defined as the temperature difference between ceramic-rich and metal-rich surfaces of the FGM shell. Due to mathematical difficulty, this section only considers linear distribution of metal and ceramic constituents, i.e. $k = 1$ and

$$K(\bar{z}) = K_m + K_{cm} \left[\frac{2(\bar{z} - R) + h}{2h} \right]. \quad (18)$$

Introduction of Eq. (18) into Eq. (17) gives temperature distribution across the shell thickness as

$$T(z) = T_m + \frac{\Delta T}{\ln \frac{K_m(R+h/2)}{K_c(R-h/2)}} \left[\ln \frac{R+z}{R-h/2} - \ln \frac{(K_c + K_m)/2 + K_{cm}z/h}{K_m} \right] \quad (19)$$

where \bar{z} has been replaced by $z + R$ after integration.

Assuming the metal surface temperature as reference temperature and substituting Eq. (19) into Eqs. (11) give $\Phi_0 = H\Delta Th$, where

$$\begin{aligned}
H = & \frac{1}{\xi - \eta} \left\{ E_m \alpha_m \left[\xi (R_h + 1/2) - \frac{\eta K_c}{K_{cm}} \right] + \frac{E_m \alpha_{cm} + E_{cm} \alpha}{2} [(R_h - 1)(1 - R_h \xi) \right. \\
& + \frac{3}{4} \xi + \frac{1}{K_{cm}^2} \left(\frac{3K_m^2 + K_c^2}{2} + 2K_m K_c (\eta - 1) - \eta K_c^2 \right) \left. \right] + E_{cm} \alpha_{cm} [-5/8 \\
& + R_h/2 - \frac{R_h^2}{3} + \xi \left(\frac{7}{24} + \frac{R_h^3}{3} - \frac{R_h^2}{2} + \frac{R_h}{4} \right) - \frac{1}{18K_{cm}^3} (11K_m^3 + 2K_c^3 (3\eta - 1) \\
& - 18\eta K_m K_c K_{cm} + 9K_m K_c (K_c - 2K_m))] \left. \right\}
\end{aligned} \tag{20}$$

and

$$R_h = R/h, \quad \xi = \ln \frac{2R_h + 1}{2R_h - 1}, \quad \eta = \ln \frac{K_c}{K_m}. \tag{21}$$

4. STABILITY ANALYSIS

In this section, an analytical approach is used to investigate the nonlinear stability of FGM cylindrical shells under mechanical and thermomechanical loads. Consider a perfect cylindrical shell with simply supported edge conditions. The boundary conditions at $x = 0, L$ are

$$w = w_{,xx} = v = u_{,x} = 0. \tag{22}$$

The approximate solution of the system of Eqs. (13) satisfying the boundary conditions (22) may be assumed as

$$\begin{aligned}
u &= U \cos \lambda_m x \sin \mu_n y \\
v &= V \sin \lambda_m x \cos \mu_n y \\
w &= W \sin \lambda_m x \sin \mu_n y
\end{aligned} \tag{23}$$

where $\lambda_m = m\pi/L$, $\mu_n = n/R$ and m, n are number of half waves in x direction and waves in y direction, respectively, and U, V, W are the amplitudes of displacements. Substitution of Eqs. (23) into Eqs. (13) and then applying Galerkin method for the resulting equations yield

$$\begin{aligned}
l_{11}U + l_{12}V + l_{13}W + n_1W^2 &= 0 \\
l_{21}U + l_{22}V + l_{23}W + n_2W^2 &= 0 \\
l_{31}U + l_{32}V + l_{33}W + n_3W^2 + n_4W^3 + n_5UW + n_6VW - \frac{P_x h \pi^2 m^2}{L^2} W \\
- \frac{\Phi_0}{1 - \nu} \left(\frac{m^2 \pi^2}{L^2} + \frac{n^2}{R^2} \right) W + \frac{16\Phi_0}{R(1 - \nu)\pi^2 mn} - \frac{16q}{\pi^2 mn} &= 0
\end{aligned} \tag{24}$$

where

$$\begin{aligned}
l_{11} &= A_{11} \frac{\pi^2 m^2}{L^2} + A_{66} \frac{n^2}{R^2}, \quad l_{12} = l_{21} = \frac{\pi mn}{LR} \left[A_{12} + A_{66} - \frac{1}{R}(B_{12} + B_{66}) \right], \\
l_{13} &= l_{31} = A_{12} \frac{\pi m}{LR} - B_{11} \frac{\pi^3 m^3}{L^3} - \frac{(B_{12} + 2B_{66}) \pi mn^2}{LR^2}, \\
l_{22} &= \left(A_{11} - \frac{2B_{11}}{R} + \frac{D_{11}}{R^2} \right) \frac{n^2}{R^2} + \left(A_{66} - \frac{2B_{66}}{R} + \frac{D_{66}}{R^2} \right) \frac{\pi^2 m^2}{L^2}, \\
l_{23} &= l_{32} = \left(A_{11} - \frac{B_{11}}{R} \right) \frac{n}{R^2} + \left(\frac{D_{11}}{R} - B_{11} \right) \frac{n^3}{R^3} + \left(\frac{D_{12} + 2D_{66}}{R} - B_{12} - 2B_{66} \right) \frac{\pi^2 m^2 n}{L^2 R}, \\
l_{33} &= D_{11} \left(\frac{\pi^4 m^4}{L^4} + \frac{n^4}{R^4} \right) + (D_{12} + 2D_{66}) \frac{2\pi^2 m^2 n^2}{L^2 R^2} + \frac{A_{11}}{R^2} - \frac{2B_{12} \pi^2 m^2}{L^2 R} - \frac{2B_{11} n^2}{R^3}, \\
n_1 &= A_{11} \frac{32\pi m^2}{9L^3 n} - \frac{16(A_{12} - A_{66})n}{9\pi LR^2}, \\
n_2 &= \left(A_{11} - \frac{B_{11}}{R} \right) \frac{32n^2}{9\pi^2 m R^3} + \left(A_{66} - A_{12} - \frac{B_{66} - B_{12}}{R} \right) \frac{16m}{9L^2 R}, \\
n_3 &= \frac{32(B_{12} - B_{66})mn}{3L^2 R^2} - \frac{16A_{12}m}{3L^2 Rn} - \frac{16A_{11}n}{3\pi^2 R^3 m}, \\
n_4 &= \frac{9A_{11}}{32} \left(\frac{\pi^4 m^4}{L^4} + \frac{n^4}{R^4} \right) + (A_{12} + 2A_{66}) \frac{\pi^2 m^2 n^2}{16L^2 R^2}, \\
n_5 &= -A_{11} \frac{32\pi m^2}{9L^3 n} - \frac{32(A_{12} - A_{66})n}{9\pi LR^2}, \\
n_6 &= \left(A_{66} - A_{12} + \frac{B_{12} - B_{66}}{R} \right) \frac{32m}{9L^2 R} + \left(\frac{B_{11}}{R} - A_{11} \right) \frac{32n^2}{9\pi^2 R^3 m}
\end{aligned} \tag{25}$$

and m, n are odd numbers. Solving the first two of Eqs. (24) for U and V yields

$$\begin{aligned}
U &= \frac{(l_{12}l_{23} - l_{22}l_{13})W + (l_{12}n_2 - l_{22}n_1)W^2}{l_{11}l_{22} - l_{12}^2} \\
V &= \frac{(l_{12}l_{13} - l_{11}l_{23})W + (l_{12}n_1 - l_{11}n_2)W^2}{l_{11}l_{22} - l_{12}^2}
\end{aligned} \tag{26}$$

Substituting Eqs. (26) into the third of Eqs. (24) we obtain

$$\frac{16q}{\pi^2 mn} = a_1 \bar{W} + a_2 \bar{W}^2 + a_3 \bar{W}^3 - \frac{P_x \pi^2 m^2}{R_h^2 L_R^2} \bar{W} + \left[\frac{16}{R_h \pi^2 mn} - \left(\frac{\pi^2 m^2}{R_h^2 L_R^2} + \frac{n^2}{R_h^2} \right) \bar{W} \right] \frac{I \Delta T}{1 - \nu} \tag{27}$$

where

$$\begin{aligned}
a_1 &= \bar{l}_{33} + \frac{2\bar{l}_{12}\bar{l}_{23}\bar{l}_{13} - (\bar{l}_{11}\bar{l}_{23}^2 + \bar{l}_{22}\bar{l}_{13}^2)}{\bar{l}_{11}\bar{l}_{22} - \bar{l}_{12}^2} \\
a_2 &= \bar{n}_3 + \frac{1}{\chi} [\bar{l}_{13} (\bar{l}_{12}\bar{n}_2 - \bar{l}_{22}\bar{n}_1) + \bar{l}_{23} (\bar{l}_{12}\bar{n}_1 - \bar{l}_{11}\bar{n}_2) + \bar{n}_5 (\bar{l}_{12}\bar{l}_{23} - \bar{l}_{22}\bar{l}_{13}) + \bar{n}_6 (\bar{l}_{12}\bar{l}_{13} - \bar{l}_{11}\bar{l}_{23})] \\
a_3 &= \bar{n}_4 + \frac{1}{\chi} [\bar{n}_5 (\bar{l}_{12}\bar{n}_2 - \bar{l}_{22}\bar{n}_1) + \bar{n}_6 (\bar{l}_{12}\bar{n}_1 - \bar{l}_{11}\bar{n}_2)]
\end{aligned} \tag{28}$$

in which

$$\begin{aligned}
\chi &= \bar{l}_{11}\bar{l}_{22} - \bar{l}_{12}^2, \\
\bar{l}_{11} &= \bar{A}_{11} \frac{\pi^2 m^2}{R_h^2 L_R^2} - \bar{B}_{11} \frac{\pi^3 m^3}{R_h^3 L_R^3} - \frac{(\bar{B}_{12} + 2\bar{B}_{66}) \pi m n^2}{R_h^3 L_R}, \\
\bar{l}_{22} &= \left(\bar{A}_{11} - \frac{2\bar{B}_{11}}{R_h} + \frac{\bar{D}_{11}}{R_h^2} \right) \frac{n^2}{R_h^2} + \left(\bar{A}_{66} - \frac{2\bar{B}_{66}}{R_h} + \frac{\bar{D}_{66}}{R_h^2} \right) \frac{\pi^2 m^2}{R_h^2 L_R^2}, \\
\bar{l}_{23} &= \left(\bar{A}_{11} - \frac{\bar{B}_{11}}{R_h} \right) \frac{n}{R_h^2} + \left(\frac{\bar{D}_{11}}{R_h} - \bar{B}_{11} \right) \frac{n^3}{R_h^3} + \left(\frac{\bar{D}_{12} + 2\bar{D}_{66}}{R_h} - \bar{B}_{12} - 2\bar{B}_{66} \right) \frac{\pi^2 m^2 n}{R_h^3 L_R^2}, \\
\bar{l}_{33} &= \bar{D}_{11} \left(\frac{\pi^4 m^4}{R_h^4 L_R^4} + \frac{n^4}{R_h^4} \right) + (\bar{D}_{12} + 2\bar{D}_{66}) \frac{2\pi^2 m^2 n^2}{R_h^4 L_R^2} + \frac{\bar{A}_{11}}{R_h^2} - \frac{2\bar{B}_{12}\pi^2 m^2}{R_h^3 L_R^2} - \frac{2\bar{B}_{11}n^2}{R_h^3}, \\
\bar{n}_1 &= \bar{A}_{11} \frac{32\pi m^2}{9R_h^3 L_R^3 n} - \frac{16n(\bar{A}_{12} - \bar{A}_{66})}{9\pi R_h^3 L_R}, \\
\bar{n}_2 &= \left(\bar{A}_{11} - \frac{\bar{B}_{11}}{R_h} \right) \frac{32n^2}{9\pi^2 m R_h^3} + \left(\bar{A}_{66} - \bar{A}_{12} - \frac{\bar{B}_{66} - \bar{B}_{12}}{R_h} \right) \frac{16m}{9R_h^3 L_R^2}, \\
\bar{n}_3 &= \frac{32mn(\bar{B}_{12} - \bar{B}_{66})}{3R_h^4 L_R^2} - \frac{16m\bar{A}_{12}}{3nR_h^3 L_R^2} - \frac{16n\bar{A}_{12}}{3m\pi^2 R_h^3}, \\
\bar{n}_4 &= \frac{9\bar{A}_{11}}{32} \left(\frac{\pi^4 m^4}{R_h^4 L_R^4} + \frac{n^4}{R_h^4} \right) + (\bar{A}_{12} + 2\bar{A}_{66}) \frac{\pi^2 m^2 n^2}{16R_h^4 L_R^2}, \\
\bar{n}_5 &= -\bar{A}_{11} \frac{32\pi m^2}{9nR_h^3 L_R^3} - \frac{32n(\bar{A}_{12} - \bar{A}_{66})}{9\pi R_h^3 L_R}, \\
\bar{n}_6 &= \left(\bar{A}_{66} - \bar{A}_{12} + \frac{\bar{B}_{12} - \bar{B}_{66}}{R_h} \right) \frac{32m}{9R_h^3 L_R^2} + \left(\frac{\bar{B}_{11}}{R_h} - \bar{A}_{11} \right) \frac{32n^2}{9\pi^2 m R_h^3}
\end{aligned} \tag{29}$$

and

$$\begin{aligned}
L_R &= L/R, \quad \bar{W} = W/h, \\
[\bar{A}_{11}, \bar{A}_{12}, \bar{A}_{66}] &= \frac{[A_{11}, A_{12}, A_{66}]}{h}, \quad [\bar{B}_{11}, \bar{B}_{12}, \bar{B}_{66}] = \frac{[B_{11}, B_{12}, B_{66}]}{h^2}, \\
[\bar{D}_{11}, \bar{D}_{12}, \bar{D}_{66}] &= \frac{[D_{11}, D_{12}, D_{66}]}{h^3}
\end{aligned} \tag{30}$$

Eq. (27) is explicit expression of external pressure-deflection curves accounting for pre-existent edge compressive and thermal loads. It is predicted that due to the presence of temperature conditions FGM cylindrical shells experience a bifurcation-type buckling behavior with buckling pressure $q_b = I\Delta T / (R_h(1 - \nu))$ (I is replaced by H in case of thermal gradient) which is independent of buckling mode (postbuckling behavior, however, is sensitive to buckling mode). In contrast, in the absence of the temperature and edge compressive force the $q(\bar{W})$ curves originate from coordinate origin and the shell undergoes bending at the onset of loading.

In a particular case which the cylindrical shell is only subjected to axial compression, Eq. (27) leads to

$$P_x = \frac{R_h^2 L_R^2}{\pi^2 m^2} (a_1 + a_2 \bar{W} + a_3 \bar{W}^2) \quad (31)$$

from which bifurcation compressive load P_{xb} is determined as

$$P_{xb} = \frac{a_1 R_h^2 L_R^2}{\pi^2 m^2} \quad (32)$$

whereas lower buckling compressive load may be obtained at $\bar{W}_0 = -a_2 / (2a_3)$ as

$$P_{xl} = P_x(\bar{W}_0) = \frac{R_h^2 L_R^2}{\pi^2 m^2} \left(a_1 - \frac{a_2^2}{4a_3} \right) \quad (33)$$

and the intensity of well-known snap-through of compressed cylindrical shells is measured by difference between bifurcation and lower buckling loads, i.e. by $a_2^2 R_h^2 L_R^2 / (4a_3 \pi^2 m^2)$.

5. RESULTS AND DISCUSSION

As part of the validation of the present approach, the buckling behavior of an isotropic thin cylindrical shell under uniform axial compressive load is analyzed, which was considered by Brush and Almroth [1] using adjacent equilibrium criterion and Donnell shallow shell theory. The dimensionless buckling axial compressive loads of a simply supported cylindrical shell are compared in Tab. 1 with result of Ref. [1]. As can be seen, a good agreement is achieved in this comparison study. Brush and Almroth's results are slightly higher than our results because the shallow shell theory, instead of improved theory, was used in their work.

Table 1. Comparison of buckling loads $P_{xcr} \times 10^3 / E$ for simply supported isotropic perfect cylindrical shell under axial compression ($\nu = 0.3$).

R/h	$L/R = 0.5$		$L/R = 1.0$		$L/R = 1.5$	
	100	150	100	150	100	150
Present	6.033(1,9) ^e	4.043(3,9)	5.954(1,7)	4.018(3,11)	6.033(3,9)	4.043(9,9)
Ref. [1]	6.087	4.047	6.063	4.035	6.087	4.047

^e The numbers in brackets indicate the buckling mode (m, n)

To illustrate the proposed approach, we consider a ceramic-metal functionally graded cylindrical shell that consists of aluminum and alumina with the following properties

$$\begin{aligned} E_m &= 70 \text{ GPa} , \alpha_m = 23 \times 10^{-6} \text{ }^\circ\text{C}^{-1} , K_m = 204 \text{ W/mK} \\ E_c &= 380 \text{ GPa} , \alpha_c = 7.4 \times 10^{-6} \text{ }^\circ\text{C}^{-1} , K_c = 10.4 \text{ W/mK} \end{aligned} \quad (34)$$

whereas Poisson's ratio is chosen to be 0.3.

Table 2. Critical buckling compressive loads P_{xcr} (in GPa) for FGM cylindrical shells, $R/h = 100$.

k	L/R			
	1.0	2.0	3.0	6.0
0	2.262(1,7) ^e	2.229(1,5)	2.262(3,7)	2.079(1,3)
0.5	1.554	1.545	1.554	1.445
1.0	1.230	1.228	1.230	1.151
5.0	0.736	0.723	0.736	0.674

^e The numbers in brackets indicate the buckling mode (m, n)

Tab. 2 considers the effects of volume fraction index k and L/R ratio on critical buckling loads P_{xcr} of FGM cylindrical shells under axial compression. As expected, the critical values of buckling loads are decreased when k increases due to drop in the volume percentage of ceramic constituent. It is also seen that critical loads are not always decreased when L/R increases.

Fig. 2 gives the effects of k on the postbuckling behavior of FGM cylindrical shells under axial compression. As can be seen, both buckling compressive loads and postbuckling load carrying capacity of cylindrical shells are reduced when k is increased. However, the increase in buckling loads and postbuckling strength is paid by a more severe snap-through phenomenon, i.e. a bigger difference between bifurcation and lower buckling loads and curves become more unstable.

Fig. 3 shows the effects of L/R ratio on the postbuckling of FGM cylindrical shells under axial compression. Although there is not much change of bifurcation point loads, buckling modes and postbuckling curves are considerably varied due to the variation of L/R ratio. Specifically, both number of waves in the circumferential direction and postbuckling bearing capability of shells are reduced when L/R is enhanced. In addition, the increase in L/R is accompanied by an unstable postbuckling behavior, i.e. a more severe snap-through response.

Figs. 4 and 5 illustrate the effects of buckling mode and pre-existent axial compressive load on the nonlinear response of FGM cylindrical shells subjected to uniform external pressure. As can be observed, for a specific buckling mode nonlinear equilibrium paths become lower and the intensity of snap-through is enhanced for higher values of

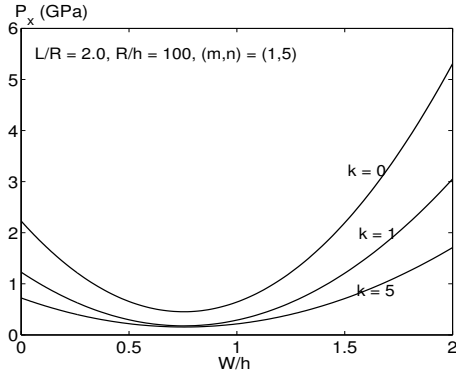


Fig. 2. Effects of k on the postbuckling behavior of FGM cylindrical shells under axial compression

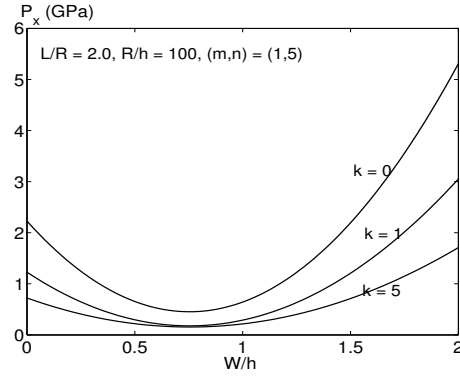


Fig. 3. Effects of L/R ratio on the postbuckling behavior of FGM cylindrical shells under axial compression

pre-existent axial compressive load. Furthermore, the cylindrical shells carry better external pressure and the nonlinear response to be more benign as the number of waves in the circumferential direction increases.

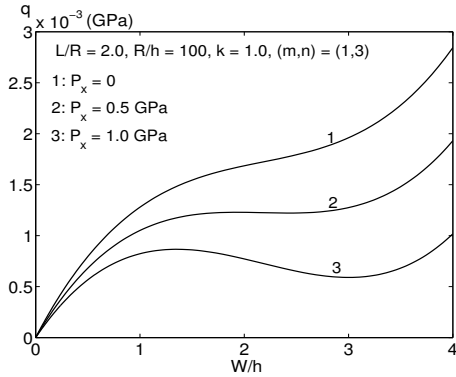


Fig. 4. Effects of pre-existent compressive load on the nonlinear response of FGM cylindrical shells under external pressure

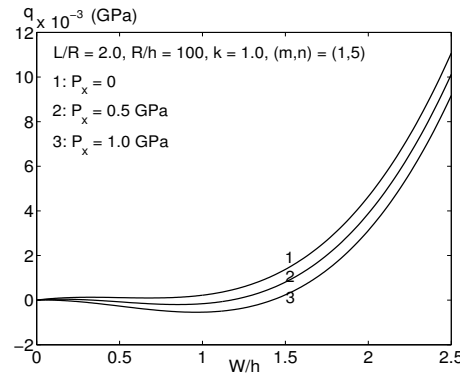


Fig. 5. Counterpart of Fig. 4 for case of $n = 5$

Figs. 6 and 7 depict the effects of environment temperature and through the thickness temperature gradient on the nonlinear response of FGM cylindrical shells under uniform external pressure in the presence of pre-existent axial compressive load. As mentioned above, due to thermal loading conditions, FGM cylindrical shells experience a bifurcation type buckling behavior. The increase in thermal loads is followed by both higher bifurcation point pressure and more severe snap-through behavior. It is interesting to note that all pressure-deflection curves go across a point for various values of temperature difference ΔT . This behavior trend of FGM shells is similar to the nonlinear response of FGM

cylindrical panels subjected to simultaneous action of external pressure and thermal loads presented in [21].

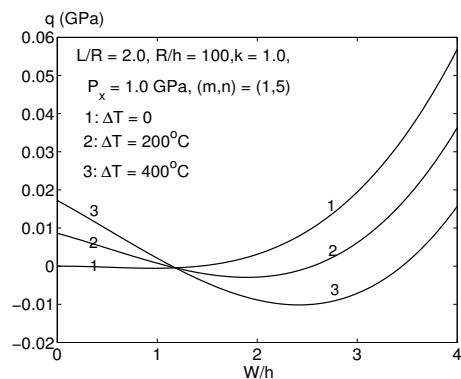


Fig. 6. Effects of the environment temperature on the nonlinear response of FGM cylindrical shells under external pressure

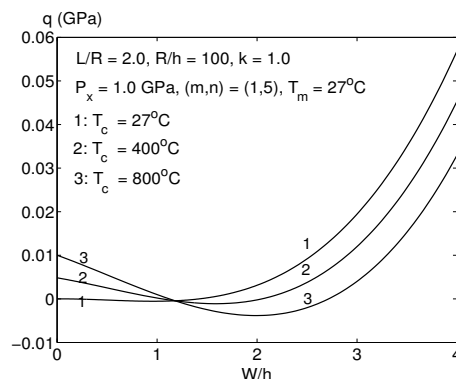


Fig. 7. Effects of the temperature gradient on the nonlinear response of FGM cylindrical shells under external pressure

6. CONCLUDING REMARKS

This paper presents an analytical approach to investigate buckling and postbuckling behaviors of FGM circular cylindrical shells subjected to axial compressive load, uniform external pressure accounting for the effects of temperature conditions. Equilibrium equations are established within the framework of improved Donnell shell theory taking into account the nonshallowness of cylindrical shell and geometrical nonlinearity. One-term approximate solution satisfying simply supported boundary conditions is assumed and explicit expressions of buckling loads and postbuckling load-deflection curves are determined by using Galerkin method. The study shows that buckling loads and postbuckling behavior of FGM cylindrical shells are greatly influenced by material and geometrical parameters and temperature conditions. The results also reveal that buckling mode and pre-existent axial compressive load have significant effects on the nonlinear response of the shells. The improved theory should be used to predict the nonlinear behavior of nonshallow cylindrical shells.

ACKNOWLEDGEMENT

This paper was supported by National Foundation for Science and Technology Development of Vietnam - NAFOSTED. The authors are grateful for this support.

REFERENCES

- [1] D.O. Brush, B.O. Almroth, *Buckling of Bars, Plates and Shells*, McGraw-Hill, New York, 1975.
- [2] V. Birman, C.W. Bert, Dynamic stability of reinforced composite cylindrical shells in thermal fields, *J. Sound and Vibration* 142(2) (1990) 183-190.

- [3] V. Birman, C. W. Bert, Buckling and postbuckling of composite plates and shells subjected to elevated temperature, *J. Appl. Mech. ASME* 60 (1993) 514-519.
- [4] M.R. Eslami, A.R. Ziaii, A. Ghorbanpour, Thermoelastic buckling of thin cylindrical shells based on improved stability equations, *J. Thermal Stresses* 19 (1996) 299-315.
- [5] S. Shahsiah, M.R. Eslami, Thermal buckling of functionally graded cylindrical shell, *J. Thermal Stresses* 26 (2003) 277-294.
- [6] R. Shahsiah, M.R. Eslami, Functionally graded cylindrical shell thermal instability based on improved Donnell equations, *AIAA Journal* 41(9) (2003) 1819-1826.
- [7] W. Lanhe, Z. Jiang, J. Liu, Thermoelastic stability of functionally graded cylindrical shells, *Compos. Struct.* 70 (2005) 60-68.
- [8] S.R. Li, R.C. Batra, Buckling of axially compressed thin cylindrical shells with functionally graded middle layer, *Thin-Walled Struct.* 44 (2006) 1039-1047.
- [9] H. Huang, Q. Han, Buckling of imperfect functionally graded cylindrical shells under axial compression, *European J. Mech., A/Solids* 27 (2008) 1026-1036.
- [10] M.M. Najafizadeh, A. Hasani, P. Khazaeinejad, Mechanical stability of functionally graded stiffened cylindrical shells, *Appl. Math. Modelling* 33 (2009) 1151-1157.
- [11] H.S. Shen, Thermal postbuckling behavior of functionally graded cylindrical shells with temperature-dependent properties, *Int. J. Solids and Struct.* 41 (2004) 1961-1974.
- [12] H.S. Shen, N. Noda, Postbuckling of FGM cylindrical shells under combined axial and radial mechanical loads in thermal environments, *Int. J. Solids and Struct.* 42 (2005) 4641-4662.
- [13] H.S. Shen, Postbuckling of axially loaded FGM hybrid cylindrical shells in thermal environments, *Compos. Sci. Tech.* 65 (2005) 1675-1690.
- [14] H.S. Shen, N. Noda, Postbuckling of pressure-loaded FGM hybrid cylindrical shells in thermal environments, *Compos. Struct.* 77 (2007) 546-560.
- [15] H. Huang, Q. Han, Nonlinear elastic buckling and postbuckling of axially compressed functionally graded cylindrical shells, *Int. J. Mech. Sci.* 51 (2009) 500-507.
- [16] H. Huang, Q. Han, Nonlinear buckling and postbuckling of heated functionally graded cylindrical shells under combined axial compression and radial pressure, *Int. J. Non-Linear Mech.* 44 (2009) 209-218.
- [17] M. Darabi, M. Darvizeh, A. Darabi, Non-linear analysis of dynamic stability for functionally graded cylindrical shells under periodic axial loading, *Compos. Struct.* 83 (2008) 201-211.
- [18] M. Shariyat, Dynamic thermal buckling of suddenly heated temperature-dependent FGM cylindrical shells under combined axial compression and external pressure, *Int. J. Solids and Struct.* 45 (2008) 2598-2612.
- [19] M. Shariyat, Dynamic buckling of suddenly loaded imperfect hybrid FGM cylindrical shells with temperature-dependent material properties under thermo-electro-mechanical loads, *Int. J. Mech. Sci.* 50 (2008) 1561-1571.
- [20] M. Shariyat, M. R. Eslami, On thermal dynamic buckling analysis of imperfect laminated cylindrical shells, *ZAMM* 80(3) (2000) 171-182.
- [21] N.D. Duc, H. V. Tung, Nonlinear response of pressure-loaded functionally graded cylindrical panels with temperature effects, *Compos. Struct.* 92 (2010) 1664-1672.

Received January 08, 2012

CONTENTS

	Pages
1. Dao Huy Bich, Nguyen Xuan Nguyen, Hoang Van Tung, Postbuckling of functionally graded cylindrical shells based on improved Donnell equations.	1
2. Bui Thi Hien, Tran Ich Thinh, Nguyen Manh Cuong, Numerical analysis of free vibration of cross-ply thick laminated composite cylindrical shells by continuous element method.	17
3. Tran Ich Thinh, Bui Van Binh, Tran Minh Tu, Static and dynamic analyses of stiffened folded laminate composite plate.	31
4. Nguyen Dinh Kien, Trinh Thanh Huong, Le Thi Ha, A co-rotational beam element for geometrically nonlinear analysis of plane frames.	51
5. Nguyen Chien Thang, Qian Xudong, Ton That Hoang Lan, Fatigue performance of tubular X-joints: Numerical investigation.	67
6. Hoang H. Truong, Chien H. Thai, H. Nguyen-Xuan, Isogeometric analysis of two-dimensional piezoelectric structures.	79
7. Pham Chi Vinh, Do Xuan Tung, Explicit homogenized equations of the piezoelectricity theory in a two-dimensional domain with a very rough interface of comb-type.	93